

# Enhanced Magnetoelastic Response near Morphotropic Phase Boundary in Ferromagnetic Materials: Experimental and Theoretical Analysis

Murtaza Adil, Sen Yang, Zhou Chao, Song Xiaoping

**Abstract**—The morphotropic phase boundary (MPB) recently has attracted constant interest in ferromagnetic systems for obtaining enhanced large magnetoelastic response. In the present study, structural and magnetoelastic properties of MPB involved ferromagnetic  $Tb_{1-x}Gd_xFe_2$  ( $0 \leq x \leq 1$ ) system has been investigated. The change of easy magnetic direction from  $\langle 111 \rangle$  to  $\langle 100 \rangle$  with increasing  $x$  up MPB composition of  $x=0.9$  is detected by step-scanned [440] synchrotron X-ray diffraction reflections. The Gd substitution for Tb changes the composition for the anisotropy compensation near MPB composition of  $x=0.9$ , which was confirmed by the analysis of detailed scanned XRD, magnetization curves and the calculation of the first anisotropy constant  $K_1$ . The spin configuration diagram accompanied with different crystal structures for  $Tb_{1-x}Gd_xFe_2$  was designed. The calculated first anisotropy constant  $K_1$  shows a minimum value at MPB composition of  $x=0.9$ . In addition, the large ratio between magnetostriction, and the absolute values of the first anisotropy constant  $|\lambda_s K_1|$  appears at MPB composition, which makes it a potential material for magnetostrictive application. Based on experimental results, a theoretical approach was also proposed to signify that the facilitated magnetization rotation and enhanced magnetoelastic effect near MPB composition are a consequence of the anisotropic flattening of free energy of ferromagnetic crystal. Our work specifies the universal existence of MPB in ferromagnetic materials which is important for substantial improvement of magnetic and magnetostrictive properties and may provide a new route to develop advanced functional materials.

**Keywords**—Free energy, lattice distortion, magnetic anisotropy, magnetostriction, morphotropic phase boundary.

## I. INTRODUCTION

MPB, a phase boundary separating two ferroelectric phases of different crystallographic symmetries in the composition temperature phase diagram [1]-[3] has drawn constant interest due to exotic magnetoelastic phenomena in the

Zhou Chao and Song Xiaoping are with the MOE Key Laboratory for Nonequilibrium Synthesis and Modulation of Condensed Matter, State Key Laboratory for Mechanical Behaviour of Materials Xi'an Jiaotong University, Xingqing Campus, Xianning West Road 28#, Beilin District, Xi'an City, Shaanxi Province, China, P.R., 710049.

Murtaza Adil and Sen Yang is with the MOE Key Laboratory for Nonequilibrium Synthesis and Modulation of Condensed Matter, State Key Laboratory for Mechanical Behaviour of Materials Xi'an Jiaotong University, Xingqing Campus, Xianning West Road 28#, Beilin District, Xi'an City, Shaanxi Province, China, P.R., 710049 (corresponding authors, e-mail: adilmurtaza@mail.xjtu.edu.cn, sen.yang@mail.xjtu.edu.cn).

This work was supported by the National Basic Research Program of China (Grant No. 2012CB619401, 51222104, 51371134, 51471125, and 51431007). This research used resources of the Advanced Photon Source, a U.S. Department of Energy (DOE) Office of Science by Argonne National Laboratory under Contract No. DE-AC02-06CH11357.

vicinity of MPB. Ferromagnetic systems are physically parallel to ferroelectrics [4] with contrast in functionalities and experimental phenomena; in ferroelectrics, polarization is a direct consequence of the local atomic displacement in the lattice, while the magnetic moment created in a ferromagnet is the result of spin orbit coupling [5]. In both systems, the order parameters are coupled to the lattice, leading to piezoelectric and magnetoelastic effect, respectively [6]. The mechanism of maximum functional responses is associated with easy path for polarization rotation in anisotropically flattened free energy profile. The effectiveness of obtaining field induced high-response via MPB in ferroelectrics has stimulated the exploration of MPB in ferromagnetic systems which are physically parallel to ferroelectrics. Recently, Yang et al. [7] reported a magnetic MPB in the  $Tb_{1-x}Dy_xCo_2$  system, proposing that MPB in ferromagnets can lead to large magnetostriction. This work was the first to emphasize that the boundary between the rhombohedral and tetragonal phases is magnetoelastic. Although its MPB composition shows enhanced magnetostriction, saturation magnetization, the Curie temperature  $T_C$  far below room temperature in this system limits its wide applications [7]. Zhou et al. [8] have reported inverse effect of MPB in system of  $Tb_{1-x}Gd_xCo_2$ , showing high magnetization, Ac susceptibility and low (near zero) magnetostriction at MPB composition  $x=0.9$ . Bergstrom et al. [9] has reported a MPB in  $Tb_{1-x}Dy_xFe_2$  (Terfenol-D), which shows large magnetostriction and high magnetic susceptibility at  $x=0.73$ . In our previous work, we have shown a newly discovered type of MPB in the ferromagnetic  $Tb_{1-x}Gd_xFe_2$  system exhibiting low magnetostriction at MPB composition  $x=0.9$  [10].

Previously reported literature reveals that in MPB involved ferromagnetic materials, enhanced magnetoelastic response near MPB composition is a consequence of the anisotropic flattening of the free energy. To understand the origin of enhanced magnetoelastic response as well as MPB in ferromagnetic system, the crystal structure, magnetic properties, spin configuration, and magnetostriction of ferromagnetic  $Tb_{1-x}Gd_xFe_2$  system are investigated. Results confirmed that the largest ratio between magnetostriction and the absolute values of the first anisotropy constant  $|\lambda_s K_1|$  appears at MPB. Furthermore, a phenomenological approach was proposed to show that the facilitated magnetization rotation and enhanced magnetoelastic phenomena are a consequence of the anisotropic flattening of the free energy profile.

## II. EXPERIMENTAL METHODS

The Polycrystalline samples of pseudobinary ferromagnetic  $Tb_{1-x}Gd_xFe_2$  ( $0 \leq x \leq 1$ ) system were prepared by method of arc-melting constituent elements (99.9% for Tb and Gd and 99.8% for Fe pure) in a high-purity argon atmosphere. The samples were remelted several times to get good homogeneity. In order to reveal the crystal structure, high-resolution synchrotron X-ray diffractometer (XRD) was employed at beamline 11-BM-B (with a strain resolution of about  $5 \times 10^{-4}$ ), Advanced Photon Source (APS), Argonne National Laboratory. For synchrotron XRD, all the samples were grounded into powders and sealed into quartz capillaries having a diameter of 0.3 mm. During the measurement, the capillary was rotated in order to average intensity as well as to minimize the preferred orientation effect. The wavelength of used X-ray was  $0.413677 \text{ \AA}$ . The field dependence magnetization (M-H) curves were measured by using superconducting quantum interference device (SQUID) magnetometer in fields up to 9 kOe. The magnetostriction was measured with standard strain gauge technique at room temperature under field of 10 kOe using a metallic strain gauge with a gauge factor of  $2.11 \pm 1\%$  attached to the center of the sample and connected to a strain indicator.

## III. RESULTS AND DISCUSSION

The step scanned [440] synchrotron XRD is shown in Fig. 1 (a). It can be seen that splitting of [440] peaks become smaller and shift to lower Bragg angles with increasing Gd content. This shows that the distortion becomes too small and the spontaneous magnetostriction decrease for the  $Tb_{1-x}Gd_xFe_2$  compounds. It is well known that spontaneous magnetostriction leads to crystal structural distortion of the compound with the cubic  $MgCu_2$ -type Laves structure below its Curie temperature. Cullen and Clark suggested that the magnetostriction in  $RFe_2$  Laves compounds is highly anisotropic [11]. A large magnetostriction exists when EMD is along  $\langle 111 \rangle$ , but the magnetostriction is small when EMD is along  $\langle 100 \rangle$ . Thus, the [440] reflection in the XRD pattern is doubly split when EMD lies along  $\langle 111 \rangle$ , while it keeps a single peak when EMD lies along  $\langle 100 \rangle$  [12], [13]. Fig. 1 (b) shows that that for  $0 \leq x \leq 0.9$ , the [440] reflections can be fitted by double peaks suggesting that the EMD of the Laves phase in those compounds lies along  $\langle 111 \rangle$ . For  $x > 0.9$ , the splitting becomes so small that the [440] reflection cannot be fitted anymore as a double-split reflection. The reflections for  $x > 0.9$  can be fitted by single peak (Fig. 1 (b)) indicating that the EMD lies along  $\langle 100 \rangle$ . These results are in good agreement with previously reported, where  $x=0, 0.5, 0.7$  the characteristic [222] reflection splits into double peaks, while [800] reflections remain unsplitting corresponding to rhombohedral symmetry with easy magnetization direction (EMD) lies along  $\langle 111 \rangle$ . For  $x=1.0$ , the characteristic [800] reflection splits into double peaks while [222] reflections remain unsplitting corresponding to tetragonal symmetry with EMD lies along  $\langle 100 \rangle$ . For  $x=0.9$ , characteristic [222] and [800] reflections split into double peaks corresponding to MPB [10].

The magnetostriction coefficient  $\lambda_{111}$  for  $Tb_{1-x}Gd_xFe_2$  compounds with  $0 \leq x \leq 0.9$  was calculated by using (1) [14], [15].

$$\lambda_{111} = 2 \frac{d_{440} - d_{4\bar{4}0}}{d_{440} + d_{4\bar{4}0}} \quad (1)$$

where  $d_{440}$  and  $d_{4\bar{4}0}$  denote the interplaner distances of the  $d_{440}$  and  $d_{4\bar{4}0}$  reflections. The magnetostriction coefficient  $\lambda_{111}$  of  $Tb_{1-x}Gd_xFe_2$  decreases from 2400 for  $TbFe_2$  to 393 for  $Tb_{0.1}Gd_{0.9}Fe_2$  and it is shown as inset of Fig. 1 (a).

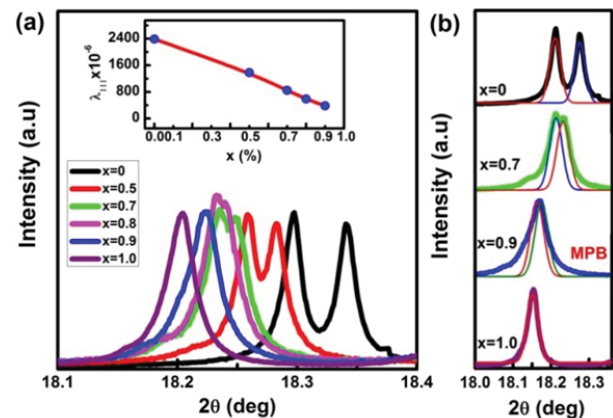


Fig. 1 (a) The step-scanned (440) synchrotron XRD for  $Tb_{1-x}Gd_xFe_2$  ( $x=0, 0.5, 0.7, 0.8, 0.9$  and  $1.0$ ). Inset shows composition dependence of the magnetostriction coefficient  $\lambda_{111}$ . (b) Double-split fittings for  $x=0, 0.7, 0.9$  and single peak fitting for  $x=1.0$

Based on analysis of synchrotron XRD data and temperature dependence of magnetization, the spin-orientation diagram in the series of  $Tb_{1-x}Gd_xFe_2$  is designed as shown in Fig. 2. Diagram shows that  $Tb_{1-x}Gd_xFe_2$  has cubic phase above  $T_c$  and rhombohedral symmetry below  $T_c$  for  $x < 0.9$  and it is changing to tetragonal symmetry with increasing Gd concentration up to  $x=0.9$ .

The magnetic field dependence of the magnetization for the  $Tb_{1-x}Gd_xFe_2$  alloys at room temperature is shown in Fig. 3 (a). It is seen that spontaneous magnetization is not saturated under applied field of 9 kOe suggesting that  $Tb_{1-x}Gd_xFe_2$  has high anisotropy. In highly anisotropic ferromagnetic materials, law of approach to saturation is widely used for the analysis of the magnetization curves of polycrystalline magnetic materials system. For this purpose, the magnetization can be written as an expansion in powers of the magnetic field as [16].

$$M = M_s \left[ 1 - \frac{a}{H} - \frac{b}{H^2} \right] \quad (2)$$

where  $M_s$  is the spontaneous saturation magnetization,  $a$  is a constant representing the contributions of inclusions and/or micro-stress,  $b$  is a constant representing the contribution of magnetocrystalline anisotropy.

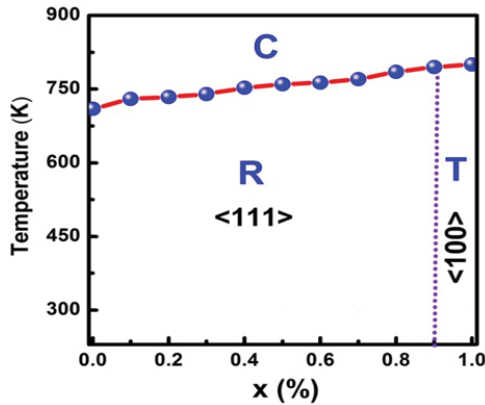


Fig. 2 Spin-orientation diagram of  $Tb_{1-x}Gd_xFe_2$  accompanied with different crystal structures for  $Tb_{1-x}Gd_xFe_2$

In the case of a ferromagnet with the cubic crystal structure, the coefficient  $b$  is given by

$$b = \frac{8}{105} \frac{K_1^2}{\mu_o^2 M_s^2} \quad (3)$$

where  $K_1$  is the cubic anisotropy constant of first order, and  $\mu_o$  is the permeability of free space. Composition dependent saturation magnetization ( $M_s$ ) is shown in Fig. 3 (b). It can be seen that  $M_s$  decreases as Gd concentration increases, and the  $M_s$  shows a peak value at MPB composition  $x=0.9$  due to easy domain switching at MPB. First magnetic anisotropy constant ( $K_1$ ) can be derived by using (3). Composition dependence of the first magnetic anisotropy constant ( $K_1$ ) derived by using (3) is shown in Fig. 3 (c). It can be seen that magnetic anisotropy first decreases with increasing Gd concentration until minimum value at MPB composition  $x=0.9$  and then increases with further increasing Gd concentration.

The magnetic field dependence of the room temperature anisotropic magnetostriction ( $\lambda_s$ ) for  $Tb_{1-x}Gd_xFe_2$  compounds is shown in Fig. 4 (a). The magnetostriction is remarkably influenced by the contribution of the Gd atom to the magnetic anisotropy of the rare-earth site. The magnetostriction decrease with the substitution of Gd for Tb under the same field from  $x=0$  to  $x=1.0$ . It is obvious that  $TbFe_2$  possesses a much larger magnetostriction than  $GdFe_2$ . This might be ascribed to the different room-temperature EMDs of these two alloys.

According to the atomic model for anisotropic magnetostriction proposed by Callen and Clark [17], a larger distortion for  $TbFe_2$  than  $GdFe_2$  indicate that the Gd ion has a lower anisotropy than that of the Tb ion because the rare-earth sublattice controls magnetostrictive properties.

The ratio between magnetostriction and the absolute value of the first anisotropy constant  $\lambda_s/|K_1|$  has been used to demonstrate the merits of a magnetostrictive material. The composition dependence of the ratio  $\lambda_s/|K_1|$  for the  $Tb_{1-x}Gd_xFe_2$  alloys is represented in Fig. 4 (b). It can be seen that every curve presents a peak at  $x=0.9$  when the magnetic field varies from 2 kOe to 10 kOe. This result further confirms that the  $Tb_{1.0}Gd_{0.9}Fe_2$  compound has a good property for

magnetostriction applications at room temperature.

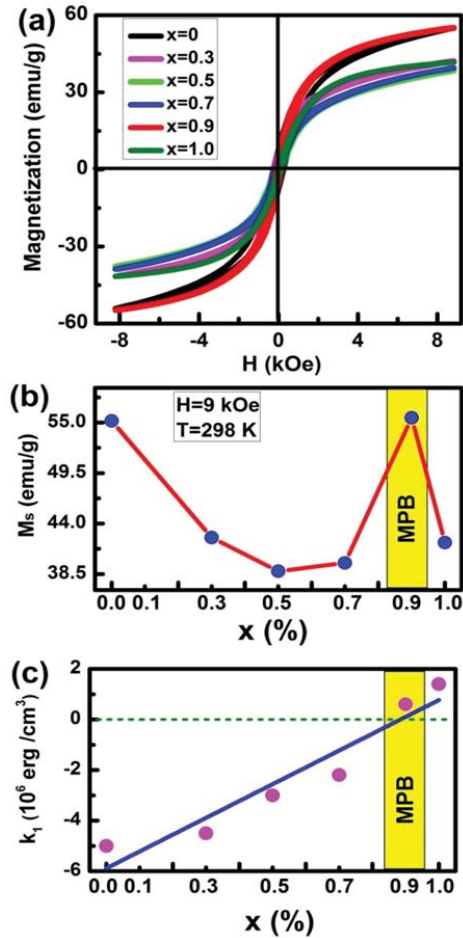


Fig. 3 (a) Hysteresis loop at room temperature under field of 9 kOe. (b) Composition dependent saturation magnetization ( $M_s$ ). (c) First anisotropy constant ( $K_1$ ) for  $Tb_{1-x}Gd_xFe_2$  system

As discussed, the enhanced magnetoelastic response appears at MPB composition of  $x=0.9$ , which is just near the spin reorientation boundary between  $\langle 111 \rangle$  and  $\langle 100 \rangle$  at room temperature. For the purpose of better understanding the origin of this enhanced magnetoelastic response near MPB in ferromagnetic system, a theoretical approach analogized to ferroelectric systems is proposed. In the following, we have theoretically demonstrated that the facilitated magnetization rotation and enhanced magnetoelastic phenomenon are a consequence of the flattening of free energy near MPB, corresponding to the free energy instability. The total free energy  $E_{tot}$  of a ferromagnetic crystal can be given as [17]-[19].

$$F_{total} = F_0 + F_a + F_e + F_{me} \quad (4)$$

where  $F_a$  is the magnetic anisotropic energy,  $F_e$  is the elastic energy, and  $F_{me}$  is the magnetoelastic energy.

The magnetic anisotropy energy  $F_a$  is given by [20]

$$F_a = K_0 + K_1(a_x^2 a_y^2 + a_y^2 a_z^2 + a_z^2 a_x^2) \quad (5)$$

where  $K_0$  and  $K_1$  are temperature-dependence anisotropic constants, and  $a_x$ ,  $a_y$ , and  $a_z$  are the direction cosines of the EMD in cubic lattice. The elastic energy  $F_e$  represented the elastic energy of the lattice due to elastic distortion  $e_{ij}$ , it is given by [18], [21].

$$F_e = \frac{1}{2}c_{11}(e_{xx}^2 + e_{yy}^2 + e_{zz}^2) + c_{12}(e_{xx}e_{yy} + e_{yy}e_{zz} + e_{zz}e_{xx}) + \frac{1}{2}c_{44}(e_{xy}^2 + e_{yz}^2 + e_{zx}^2) \quad (6)$$

where  $c_{11}$ ,  $c_{12}$ , and  $c_{44}$  are the elastic modulus and the  $e_{ij}$  represents the elastic distortion tensor. The magnetoelastic energy  $F_{me}$ , arising from the strain dependence of the anisotropy, can be described as [21].

$$F_{me} = B_1[e_{xx}(a_x^2 - \frac{1}{3}) + e_{yy}(a_y^2 - \frac{1}{3}) + e_{zz}(a_z^2 - \frac{1}{3})] + B_2(e_{xy}a_xa_y + e_{yz}a_ya_z + e_{zx}a_zax) \quad (7)$$

where  $B_1$  and  $B_2$  are the magnetoelastic coupling coefficients and determined by the elastic modulus  $c_{ij}$ ,  $\lambda_{100}$ , and  $\lambda_{111}$  in this form [17], [21].

$$B_1 = -\frac{3}{2}\lambda_{100}(c_{11} - c_{12}) \quad (8)$$

$$B_2 = -3\lambda_{111}c_{44}$$

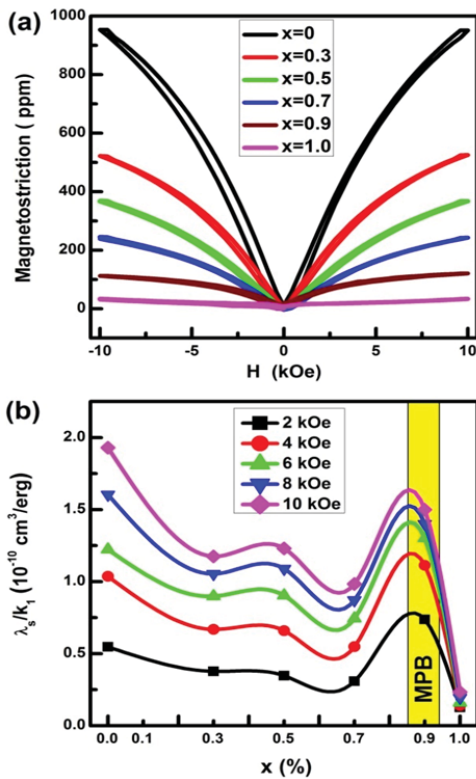


Fig. 4 (a) Magnetostriction ( $\lambda_s$ ) for polycrystalline  $Tb_{1-x}Gd_xFe_2$  alloys at room temperature under  $H=10kOe$ . (b) Composition dependence of the ratio  $\lambda_s/|K_1|$  for the  $Tb_{1-x}Gd_xFe_2$

Minimizing the total free energy with respect to all independent strains  $e_{ij}$ ,  $(\partial F/\partial e_{ij})$  yields a spontaneous lattice distortion  $(e_{ij})_s$  to the initial cubic lattice

$$e_{xx} = -\frac{B_1}{c_{11} - c_{12}}(a_x^2 - \frac{1}{3})$$

$$e_{xy} = -\frac{B_2}{c_{44}}(a_xa_y)$$

$$e_{yy} = -\frac{B_1}{c_{11} - c_{12}}(a_y^2 - \frac{1}{3}) \quad (9)$$

$$e_{yz} = -\frac{B_2}{c_{44}}(a_ya_z)$$

$$e_{zz} = -\frac{B_1}{c_{11} - c_{12}}(a_z^2 - \frac{1}{3})$$

$$e_{zx} = -\frac{B_2}{c_{44}}(a_zax)$$

Substituting these values into (4)  $E_{total}$ , the total energy can be described as

$$F_{total} = F_0 + (K_1 + \frac{B_1^2}{c_{11} - c_{12}} - \frac{B_2^2}{2c_{44}})(a_x^2a_y^2 + a_y^2a_z^2 + a_z^2a_x^2) \quad (10)$$

$$F_{total} = F_0 + [K_1 + \frac{9}{4}(c_{11} - c_{12})\lambda_{100}^2 - \frac{9}{2}c_{44}\lambda_{111}^2](a_x^2a_y^2 + a_y^2a_z^2 + a_z^2a_x^2) \quad (11)$$

In order to expediently expose the anisotropic magnetization process in  $Tb_{1-x}Gd_xFe_2$ , Fig. 5 (a) schematically shows the different easy magnetization orientations in the cubic principal axis space.

We might as well suppose the initial spontaneous magnetization along the [111] axis. When external disturbance such as external magnetic field is applied, strength and direction of magnetization will be affected, accompanying with the lattice distortion as suggested in last part. In the former case,  $a_x$ ,  $a_y$ , and  $a_z$  change by the same amount, corresponding to the enhancement of magnetization along [111], while the crystal structure remains rhombohedral. We can simply call this case as  $[M_{RR}]$ . In the latter case, considering the symmetry of (11), a tetragonal distortion will be induced in the crystal and magnetization rotates along the [111]-[001] (from R to T) path.

For simple, we name the rotation of [111]-[001] as  $[M_{RT}]$ . energy change for the different cases, which is respectively named as  $\Delta E = M_{RR}$ , and  $\Delta E = M_{RT}$  can be calculated by using (11) if elastic modulus and the first anisotropy constant are inserted. The positions of rhombohedral, tetragonal, and cubic phases, as well as the paths can be indicated. For an easier comparison, the  $a_x$  dependence of free energy profiles  $\Delta E^{[R-T]}$  for different compositions  $x=0,0.3,0.5,0.7$  and  $0.9$  is shown in Fig. 5 (b).

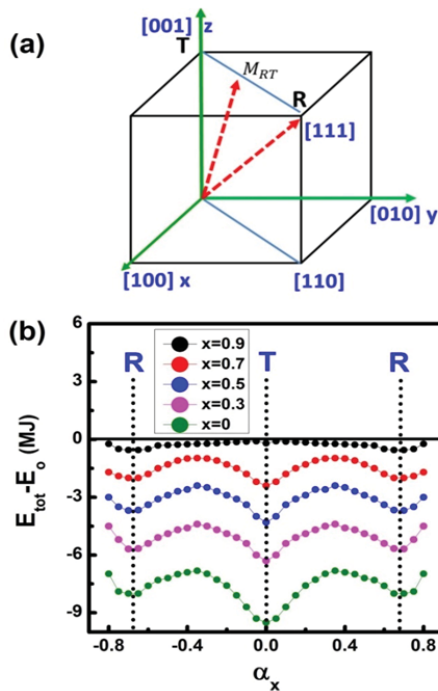


Fig. 5 (a) Magnetization in the cubic coordinate system and different monoclinic magnetization paths R and T, represent magnetization direction of, [111] (rhombohedral) and [100] (tetragonal) respectively.  $[M_{RT}]$  describe magnetization rotation paths of [111]- [001]. (b)  $\alpha_x$  dependence of free energy  $\Delta E$  profiles for different compositions. R and T represent magnetization direction of [111] (rhombohedral) and [100] (tetragonal), respectively

Comparing  $\Delta E = M_{RR}$  and  $\Delta E = M_{RT}$ , an evident conclusion could be made that the energy profiles  $\Delta E = M_{RT}$  is the least flat for the MPB composition. The meaning of this is that an MPB composition of  $Tb_{0.1}Gd_{0.9}Fe_2$  corresponds to the weakest magnetic anisotropy. This weak magnetization anisotropy yields a low barrier for the transition between  $\langle 111 \rangle R$  and  $\langle 100 \rangle T$  magnetization states. Therefore, the magnetization state would be changed easily when a lower magnetic field is applied. It is well accepted that in  $RFe_2$  compounds magnetostriction is contributed by the 4f electrons of RE. Due to the spin-orbit coupling, large additional magnetoelastic energy appears. Furthermore, the atoms surrounding the 4f shell feel a modified Coulomb interaction and will attain new equilibrium positions. As a consequence, a large strain will appear under a relatively low applied field. Similar to the theoretical analysis based on Landau-Ginsburg-Devonshire theory in ferromagnetic material, this energy flat leads to phase coexistence as well as the magnetic softening and the enhanced magnetoelastic response.

#### IV. CONCLUSION

In conclusion, the effects of Gd substitution for Tb on the structure, magnetic transition, and magnetostriction properties of the pseudobinary  $Tb_{1-x}Gd_xFe_2$  compounds have been investigated. The analysis of step scanned XRD and the spin reorientation together with the largest  $|\lambda_g/K_1|$  confirmed that the low anisotropy could be reached at MPB composition of  $x=0.9$ .

The spin configuration diagram accompanied with different crystal structures for  $Tb_{1-x}Gd_xFe_2$  was also constructed. A theoretical analysis showed that the least energy flat corresponding to a low energy barrier for magnetization rotation and enhanced magnetoelastic response near MPB in ferromagnetic  $Tb_{1-x}Gd_xFe_2$  system which could make it potential material for magnetostrictive application.

#### ACKNOWLEDGMENT

One of us (Murtaza Adil) would like to grateful to Ms. Sadaf Noreen (Government College University, Faisalabad, Pakistan), Muhammad Tahir khan, Awais Ghani and Muhammad Sadiq Fareed (Xi'an Jiaotong University) for helpful discussions.

#### REFERENCES

- [1] B. Jaffe, W.R. Cook, H. Jaffe, *Piezoelectric Ceramics* (Academic). New York: 1971.
- [2] K. Uchino, *Ferroelectric Devices* (Marcel Dekker). New York: 2000.
- [3] Ahart M, Somayazulu M, Cohen RE, Ganesh P, Dera P, Mao HK, Hemley RJ, Ren Y, Liermann P, Wu Z, "Origin of morphotropic phase boundaries in ferroelectrics". *Nature.*, vol. 451, Jan. 2008, pp. 545-8.
- [4] V.K. Wadhawan, *Introduction to Ferroic Materials*, Gordon and Breach, Amsterdam: 2000.
- [5] N. A. Spaldin *Analogies and differences between ferroelectrics and ferromagnets. In Physics of Ferroelectrics*, Springer Berlin Heidelberg: 2007. pp. 175-218.
- [6] R. E. Newnham. "Phase transformations in smart materials". *Acta Crystallographica Section A: Foundations of Crystallography.*, vol. 54, Nov. 1998, pp.729-37.
- [7] S. Yang, H. Bao, C. Zhou, Y. Wang, X. Ren, Y. Matsushita et.al, "Large Magnetostriction from Morphotropic Phase Boundary in Ferromagnets". *Physical review letters.*, vol.104, May .2010, pp. 197201.
- [8] C. Zhou, S. Ren, H. Bao, S. Yang, Y. Yao, Y. Ji, X. Ren, Y. Matsushita, Y. Katsuya, M. Tanaka, K. Kobayashi. "Inverse effect of morphotropic phase boundary on the magnetostriction of ferromagnetic  $Tb_{1-x}Gd_xCo_2$ ". *Physical Review B.*, vol. 89, Mar .2014, pp.100101.
- [9] J. R. Bergstrom, M. Wuttig, J. Cullen, P. Zavalij, R. Briber, C. Dennis, V. O. Garlea, M. Laver. "Morphotropic Phase Boundaries in Ferromagnets:  $Tb_{1-x}Dy_xFe_2$  Alloys." *Physical review letters.*, vol. 111, Jul .2013, pp. 017203.
- [10] M. Adil, S. Yang, M. Mi, C. Zhou, J. Wang, R. Zhang, X. Liao, Y. Wang, X. Ren, X. Song, Y. Ren. "Morphotropic phase boundary and magnetoelastic behaviour in ferromagnetic  $Tb_{1-x}Gd_xFe_2$  system. Applied Physics Letters., vol. 106, Mar. 2015, pp.132403.
- [11] J. R. Cullen and A. E. Clark, "Magnetostriction and structural distortion in rare-earth intermetallics". *Phys. Rev. B.*, vol. 15, May, 1977, pp. 4510S.
- [12] W. J. Ren, Z. D. Zhang, X. P. Song, X. G. Zhao, and X. M. Jin, "Composition anisotropy compensation and spontaneous magnetostriction in  $Tb_{0.2}Dy_{0.8-x}Pr_x(Fe_{0.9}B_{0.1})_{1.93}$  alloys". *Appl. Phys. Lett.*, vol. 82, Apr .2003, pp. 2664.
- [13] A. E. Dwight and C. W. Kimball, "TbFe<sub>2</sub>, a rhombohedral Laves phase". *Acta Crystallogr. Sect. B: Struct. Crystallogr. Cryst. Chem.*, vol. 30, Nov.1974, pp. 2791.
- [14] W. J. Ren, Z. D. Zhang, A. S. Markysan, X. G. Zhao, X. M. Jin and X. P. Song, "The beneficial effect of the boron substitution on the magnetostrictive compound  $Tb_{0.7}Pr_{0.3}Fe_2$ ". *J. Phys. D.* vol. 34, Oct. 2001, pp. 3024.
- [15] E. Gratz, A. Lindbaum, A. S. Markosyan, H. Mueller, and A. Y. Sokolov, "Isotropic and anisotropic magnetoelastic interactions in heavy and light RCo<sub>2</sub> Laves phase compounds." *J. Phys.: Condens. Matter.*, Aug. 1994, vol.4, pp. 6699.
- [16] S. Chikazumi, *Physics of Ferromagnetism*, ed. 2nd. New York: 1997, p. 503.
- [17] A.E. Clark, in: E.P. Wohlfarth (Ed.), *Ferromagnetic Materials*, vol. 1, North- Holland:1980, p. 531-589.
- [18] K. Kittel, "Physical theory of ferromagnetic domains", *Rev. Mod. Phys.*, Oct.1949, vol. 21, pp. 54.

- [19] K. H. Ahn, T. Lookman, and A. R. Bishop, "Strain-induced metal-insulator phase coexistence in perovskite manganites" *Nature (London)*, Mar.2004, vol. 428, pp. 401.
- [20] N. S. Akulov, "Magnetostriction of Iron Crystals", *Z. Phys.*, vol.52, Nov.1928, pp.389.
- [21] R. C. O'Handley, *Modern Magnetic Materials: Principles and Applications*, Wiley, New York: 2000.